Received: 23 September 2019 | Accepted: 28 January 2020

DOI: 10.1002/sctm.19-0316

TISSUE ENGINEERING AND REGENERATIVE MEDICINE

STEM CELLS TRANSLATIONAL MEDICINE

Functional restoration of ex vivo model of pylorus: Coinjection of neural progenitor cells and interstitial cells of Cajal

Prabhash Dadhich[1,2] | **Khalil N. Bitar**[1,2,3,4]

[1]Wake Forest Institute for Regenerative Medicine, Wake Forest School of Medicine, Winston-Salem, North Carolina

[2]Program in Neuro-Gastroenterology and Motility, Wake Forest School of Medicine, Winston-Salem, North Carolina

[3]Section on Gastroenterology, Wake Forest School of Medicine, Winston-Salem, North Carolina

[4]Virginia Tech-Wake Forest School of Biomedical Engineering and Sciences, Wake Forest School of Medicine, Winston-Salem, North Carolina

Correspondence
Khalil N. Bitar, PhD, AGAF, Wake Forest Institute for Regenerative Medicine, Winston-Salem, NC 27101.
Email: kbitar@wakehealth.edu

Funding information
Wake Forest School of Medicine; NIH/NIDDK STTR, Grant/Award Number: R42DK105593

Abstract

Transplantation of neural stem cells is a promising approach in treatment of intestinal dysfunctionality. The interstitial cells of Cajal (ICCs) are also critical in conditions such as pyloric dysfunctionality and gastroparesis. The objective of this study was to replenish neurons and ICCs in a dysfunctional pylorus as cell-based therapy to restore functionality. ICCs and enteric neural progenitor cells (NPCs) were isolated from rat duodenum and transduced with fluorescent proteins. Rat pylorus was harvested, and an ex-vivo neuromuscular dysfunctional model was developed by selective ablation of neurons and ICCs via chemical treatments. Cellular repopulation and restoration of motility were assessed by immunohistochemistry, qPCR, and functional analysis after delivery of fluorescently tagged cells. Chemical treatment of pylorus resulted in significant depletion of ICCs (67%, $P = .0024$; n = 3) and neural cells (83%, $P = .0012$; n = 3). Delivered ICCs and NPCs survived and integrated with host muscle layers. Coinjection of ICCs with NPCs exhibited 34.4% ($P = .0004$; n = 3) and 61.0% ($P = .0003$; n = 3) upregulation of ANO1 and βIII tubulin, respectively. This regeneration resulted in the restoration of agonist-induced excitatory contraction (82%) and neuron evoked relaxation (83%). The functional studies with specific neuronal nitric oxide (NO) synthase blocker confirmed that restoration of relaxation was NO mediated and neuronally derived. The simultaneous delivery of ICCs observed 35.7% higher neuronal differentiation and functional restoration compared with injection of NPCs alone. Injected NPCs and ICCs integrated into the dysfunctional ex vivo pylorus tissues and restored neuromuscular functionality. The co-transplantation of NPCs and ICCs can be used to treat neurodegenerative disorders of the pylorus.

KEYWORDS

cell interactions, cell transplantation, cellular therapy, differentiation, experimental models, neural differentiation, tissue regeneration

1 | INTRODUCTION

Gastroparesis is a symptomatic motility disorder characterized by delayed gastric emptying without any physical barrier. The common symptoms include epigastric pain, early satiety, postprandial fullness, with nausea, and vomiting.[1,2] In an age-adjusted study, the prevalence of definite gastroparesis per 100 000 persons was 9.6 (95% confidence interval [CI], 1.8-17.4) in men and 37.8 (95% CI, 23.3-52.4) in

women (approximately four times higher than men).[3] The etiology of gastroparesis is complex, with the reduction of interstitial cells of Cajal (ICCs) and the disappearance and disorganization of neuronal nitric oxide synthase (nNOS) cells in the stomach most common.[1,4-6] Inhibitory nitrergic neurons are responsible for relaxation of smooth muscle via nitric oxide (NO) secretion, resulting in accommodation of the fundus, relaxation of the pylorus, and peristaltic reflex of the small intestine.[7,8] NO appears to be a survival factor for ICCs as well. It was evident in a study, where 50% to 70% of myenteric-ganglia-related ICCs were decreased in all $nNOS^{-/-}$ mice and later increased by NO donors.[9] Furthermore, the loss of nNOS and ICCs affects the activity and endurance of smooth muscle cells (SMCs) as well.[4,6]

Currently, the standard treatment options for gastroparesis ranges from cholinergic agents, metoclopramide, botulinum toxin injections, implantation of gastric electrical stimulators,[10] total parenteral nutrition to pyloroplasty, vagotomy, myotomy, and gastrectomy.[1,2,11] The current treatments are palliative solutions and inadequate for the long-term relief in gastroparesis.

In this context, regenerative medicine offers an alternative method, where direct cell delivery may provide an efficient and enduring solution to gastrointestinal motility disorders. In a recent cell transplantation report, neonatal gut-derived neural crest progenitors reconstructed the ganglionic function in benzalkonium chloride (BAC)-treated homogenic rat colon.[12] In another study, transplanted progenitors generated functional neurons in the postnatal colon.[13,14] Central nervous system (CNS)-derived neural stem cells survived after transplantation into pylorus of mice.[15] Different studies have reported survival and functional differentiation of various stem/progenitor cells in the embryonic gut or postnatal colon; however, it is not yet known whether the enteric nervous system (ENS)-derived adult NPCs can migrate, proliferate, and generate functional neurons in the postnatal pylorus. Moreover, ICCs are another critical factor in neuromuscular dysfunction and essential for long-term restoration of the neuronal functionality of pylorus.

In the present study, the objective was to evaluate the effect of co-transplantation of ENS-derived adult NPCs and ICCs in a gastroparesis model. In the present study, an ex vivo neuromuscular dysfunction pylorus was developed by selective depletion of neurons and ICCs. The ENS derived NPCs, and ICCs injected to the ex vivo neuromuscular dysfunction pylorus to restore and repopulate the cell population. Cell survival, differentiation, and functional restoration were evaluated and compared with native tissues.

Significance statement

In regenerative medicine, it is possible to use the patient's own interstitial cells of Cajal (ICCs) and neural progenitor cells (NPCs) to be injected into the pylorus as cellular therapy. The functional ex vivo diseased model of the pylorus was developed, and ICCs and NPCs delivered as treatments for neuromuscular dysfunctionality. Detailed quantitative and qualitative analysis confirmed reinstatement and restoration of functionality. The current preliminary study with the ex vivo diseased model proposed the next level of cell therapy for the treatment of gastroparesis.

2 | MATERIALS AND METHODS

2.1 | Experimental design

NPCs and ICCs were isolated from the duodenum and fluorescently tagged with cyan fluorescent protein (CFP) and green fluorescent protein (GFP), respectively. An ex vivo dysfunctional pylorus model was developed via treatment with BAC and imatinib mesylate (IM). The NPCs and ICCs were delivered intramusclular and evaluated for cell survival, integration, and physiological functionality. The in vivo experiments were carried out on euthanized rats after endpoint of another study. The animal experiments were reviewed and approved by the Institutional Animal Care and Use Committee at the Wake Forest School of Medicine.

2.2 | Reagents

Cell culture reagents were obtained from Life Technologies (Grand Island) unless specified otherwise. Neural growth media consisted of neurobasal, 1 × N2 supplement, recombinant human epidermal growth factor, recombinant basic fibroblast growth factor. Neural differentiation media consisted of Neurobasal-A supplemented with 2% fetal bovine serum (FBS), 1×B27 supplement. ICC growth media consisted of Dulbecco's modified Eagle's medium (DMEM) with 10% FBS, 2 mM L-glutamine, and stem cell growth factor. All the media supplemented with 1× antibiotic-antimycotic. Tetrodotoxin (TTX) and N_{ω}-nitro-L-arginine methyl ester hydrochloride (L-NAME) were purchased from Sigma (St. Louis, Missouri).

2.3 | Cell isolation

Both NPCs and ICCs were isolated from duodenum of the rat as previously described.[16] The biopsies were washed thrice with HBSS (with 2× antibiotic-antimycotic solution) followed by mincing. Then biopsies were divided into two parts for separate isolation of NPCs and ICCs.

2.3.1 | Isolation of enteric NPCs

Minced tissues were digested twice for an hour each, in a mixture of 0.85 mg/mL type II collagenase, 0.85 mg/mL dispase II, and 20 μL/mL DNAse-1 in DMEM. The digested tissues washed and passed through 70 and 40 μm nylon cell strainer before incubation at 37°C in a 7% CO_2. The isolated cells stained positive for neural crest-derived cell marker $p75^{NTR}$ and nestin.

2.3.2 | Isolation of ICCs

The minced biopsies were digested using a mixture of type II collagenase, bovine serum albumin, trypsin inhibitor, with adenosine triphosphate for 1 hour. The digested tissues were washed and plated into collagen (2.5 μg/mL; Falcon/BD, Franklin Lakes, New Jersey) coated plates, incubated at 37°C in a 5% CO_2. The isolated cells were characterized for ANO1-positive marker.

2.4 | Cell transfection

The NPCs and ICCs were transduced with lentiviral particles for CFP and GFP, respectively (GeneCopeia, Rockville, Maryland) followed by puromycin treatment to select stably transduced cells. The transfection was quantified using fluorescence-activated cell sorting (FACS).

2.4.1 | Development of ex vivo neuromuscular dysfunctional pylorus

The rat (1-year old; n = 3) pylorus was harvested, cleaned, cut into two parts, and pinned on Sylgard-coated dishes. One piece of the pylorus (control group) was treated with phosphate-buffered saline (PBS), whereas the experimental group was treated with a mixture of 0.9% BAC and 1.2 mM of IM (1:1 ratio). The treated tissues were washed and incubated in smooth muscle growth media at 37°C with 5% CO_2.

2.5 | Delivery of transduced cells to ex vivo neuromuscular dysfunctional pylorus

Each BAC + IM-treated pylorus was divided into three parts. (a) injection of CFP-NPCs (NPCs group); (b) injection of CFP-NPCs and GFP-ICCs (NPC + ICC group), and (c) normal saline without any cells (BAC + IM-treated tissue).

The GFP-ICCs and CFP-NPCs were harvested, counted, and 1×10^4 cells/μL suspended in normal saline following washing. The cells were delivered via multipoint injections using a hypodermic syringe (22 gauge) into the myenteric plexus layer of the pylorus tissue (100 μL; 1×10^6 cells of each type). After injection, the tissues were placed into separate culture wells in neural differentiation media and incubated at 37°C with 5% CO_2.

2.6 | Assessment of cell survival, differentiation, and functional restoration

2.6.1 | Microscopic characterization

Cell survival and differentiation were evaluated via immunohistochemical studies. After 15 days of incubation, tissue was fixed, embedded, sectioned, and processed for staining. The tissue integrity was evaluated via hematoxylin and eosin (H&E). The tissues were stained for neural cell differentiation markers beta-III tubulin (βIII-tub; polyclonal antiserum, 1:200), nNOS (polyclonal antiserum, 1:200), and ICC markers such as ANO1 (polyclonal antiserum, 1:200) to characterize the survival and restoration of neurons and ICCs in the tissues. The Nikon Eclipse Ti inverted microscope was used for observation and image acquisition.

2.6.2 | Biological characterization

Cell survival and differentiation were quantified via genetic expressions of beta-III tubulin, ANO1, nNOS, choline acetyltransferase (ChAT) using quantitative reverse transcriptase-polymerase chain reaction (qRT-PCR). RNA was extracted using Qiagen RNeasy Mini Kit (Qiagen, Valencia, California), and the complementary DNA (cDNA) was prepared with 2 μg of RNA using high-capacity cDNA Reverse Transcription Kits (Applied Biosystems, California). Around 50 ng of cDNA was used to perform qPCR studies using 2 μL of premixed primers and 10 μL of PowerUp SYBR Green master mix (ThermoFisher Scientific, California) at 7300 Real-Time PCR System (Applied Biosystems). The GAPDH and 18s-ribosomal kept as the housekeeping gene and ANO1, beta-III tubulin, nNOS, and ChAT were target genes. Resulting protein expression was normalized to the housekeeping gene, and the average expression fold change was calculated with the standard gene.

2.6.3 | Physiological functional characterization

Tissues were analyzed for physiological functionality before and after cell delivery. Tissues were hooked in a horizontal tissue bath (F10; Harvard Apparatus, Holliston, Massachusetts). Force data were acquired using LabChart 7 software (AD Instruments, Colorado Springs, Colorado). The spontaneous basal tone was measured. Contraction and relaxation were evaluated with the addition of acetylcholine (ACh; 1 μM) and electrical field stimulation (EFS; 5 Hz, 0.5 milliseconds), respectively. Pretreatment with TTX (1 μmoL/L; voltage-gated Na + nerve channels blocker) and L-NAME (300 μM; nNOS inhibitor) were carried out to validate neo-innervation. The ICC activity was evaluated by pretreatment of tissues with TMEM16A-inhibitor (T16; 10 μM), ICC-specific calcium-activated chloride channel blocker.

2.7 | Statistical analysis

All the studies were carried out in triplicates, statistically analyzed by two-tailed Student's *t*-test, and data represented mean ± SE unless noted otherwise. One-way analysis of variance was performed with Bonferroni post hoc analysis for statistical significance of differences between the experimental groups. The correlation between different time interval studies was determined using Pearson's correlation coefficient. Longitudinal functional outcomes within a group were compared using the Wilcoxon test and reconfirmed with paired T-test

following normalization. All authors had access to the study data, reviewed and approved the final manuscript.

3 | RESULTS

3.1 | Isolation, tagging, and characterization of NPCs

NPCs were isolated from duodenum biopsies (150 ± 20 μg, n = 5) using a previously described method.[16] The circular shaped cell bodies proliferated in suspension condition, formed clusters known as neurospheres. The isolated NPCs were successfully transfected with fluorescent stable CFP lentiviral particles (with puro selection marker) using spinoculation method. The stably transduced cells successfully expressed cyan fluorescence under microscope (Figure 1A), quantitatively 98.5% ± 1% positive under FACS. Isolated NPCs were positive for both nestin (Figure 1B) and $p75^{NTR}$ (Figure 1C). The image analysis (ImageJ software) confirmed that 90% ± 3% and 95% ± 2% cells were positive for $p75^{NTR}$ and nestin, respectively. The cellular properties (viability, proliferation; methods are in Appendix S1) were unaffected after transfection. The rate of cell proliferation was consistent between transfected and non-transfected cells. (Figure 1G). The cells were >95% ± 2% viable, and an average rate of proliferation was consistent up to five generations (92.3% ± 1.5%).

3.2 | Isolation, tagging, and characterization of ICCs

The ICCs were successfully isolated from duodenum and displayed characteristic fusiform cell bodies with prominent nuclei (Figure 1D). The ICCs were tagged with fluorescent stable GFP lentiviral particles (with puro selection marker). The stably transduced cells after puromycin selection displayed green fluorescence under the microscope (Figure 1E) were quantitatively 97.5% ± 2% positive during FACS. The cells were 97.5% ± 2% positive for the $Ca^{(2+)}$-activated $Cl^{(-)}$ channel cell marker ANO1 (TMEM16A) (Figure 1F). The isolated cells were negative for the smoothelin (data not shown). The reactivity against ANO1 was further validated via qPCR (Figure 1I). Isolated cells positively expressed ANO1, without any significant differences for three generations (Figure 1). The viability and rate of cell proliferation were

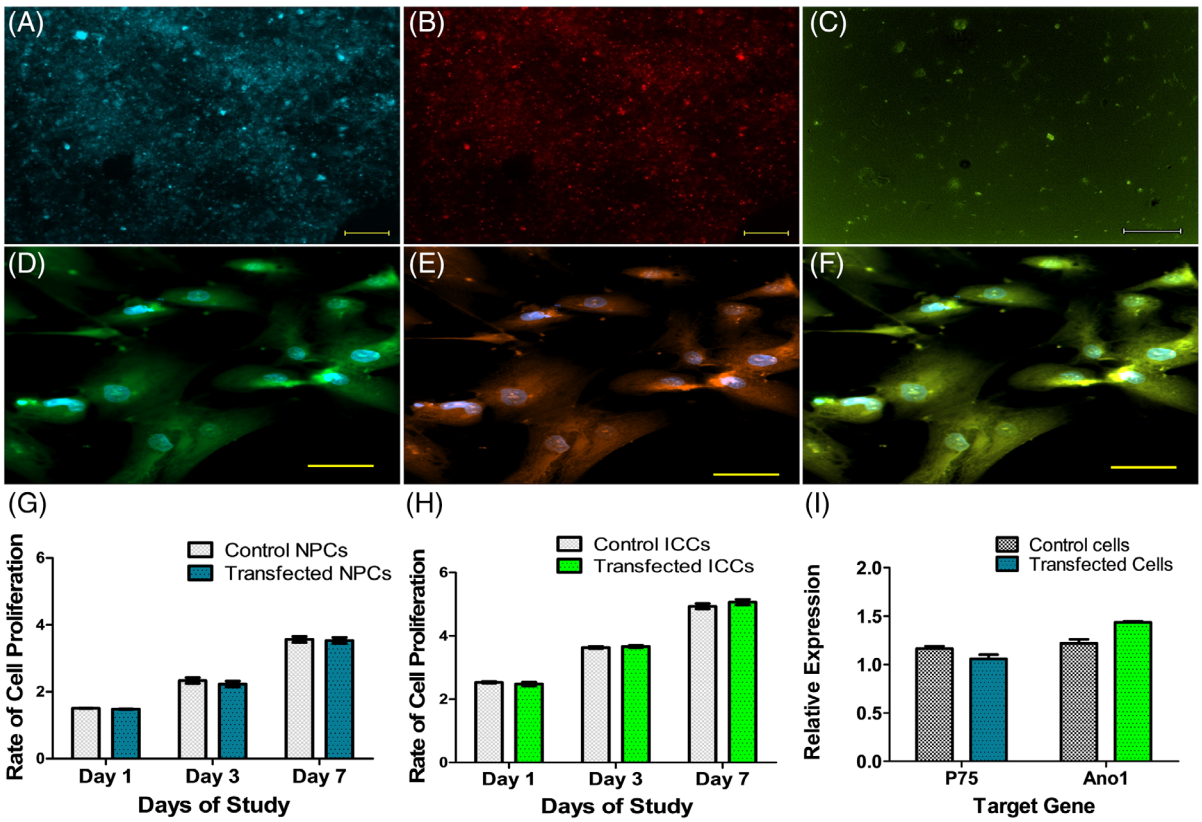

FIGURE 1 Immunocytochemical characterization of isolated enteric NPCs and ICCs from rat pylorus. A, Immunofluorescent images showing that CFP-transduced NPCs were exhibited characteristic; B, nestin and C, $P75^{NTR}$ immunoreactivity; D, GFP-transfected ICCs with apparent nucleus and triangular cell body with thin, moniliform processes; E, characteristic immunoreactivity of transfected ICCs with Ano1 F, merged image. The graphs represented no significant difference in cell proliferation kinetics after transfection of G, NPCs and H, ICCs. I, The graph represents no significant difference in genetic expression of P75 and ANo1 after transfection of NPCs and ICCs, respectively ($P < .05$, n = 3); scale bar 100 μm. CFP, cyan fluorescent protein; GFP, green fluorescent protein; ICC, interstitial cells of Cajal; NPC, neural progenitor cell

consistent up to three generation as >96.2% ± 3% and 94.3% ± 3.5% (Figure 1H), respectively.

3.3 | Development of ex vivo tissue model for neuromuscular dysfunctional pylorus

The application of BAC is a standard method to induce denervation in a tissue (in vivo and ex vivo) and the development of gastroparesis tissue model for research.[12,14,17] This method of denervation does not affect ICCs.[17] BAC was combined with IM, a c-Kit inhibitor, to target ICCs. There was 0.9% BAC, and 1.2 mM of IM was optimized to cause maximum denervation and ICCs depletion, without affecting the SMCs. The time of BAC + IM treatment was also optimized for 1 hour. The higher concentration of BAC + IM solution and longer exposure of treatment affected the serosal integrity and SMCs viability (data not shown).

3.4 | Characterization of ex vivo tissue model for dysfunctional pylorus

3.4.1 | Microscopic characterization

H&E-stained sections demonstrated the constitution of four distinct layers of the pylorus (Figure 2). A continual and intact serosa in all the tissues confirmed that BAC + IM did not affect the structural integrity of the outer layer (Figure 2).

Immunostaining of PBS-treated tissues displayed continuous, reticulated neuronal network with βIII-tub (Figure 2B), nNOS neuronal network (Figure 2C), and multiple connected fusiform ICCs bodies with ANO1 (Figure 2D). BAC + IM-treated tissues displayed poor immunereaction and confirmed the decrease of the neuronal (Figure 2F), nNOS (Figure 2G), and population ICCs (Figure 2H). The semi-quantitative histomorphometric analysis of the sections resulted in 70% and 86% reduction in ANO1 and βIII-tub (n = 3, P = .015) reactivity.

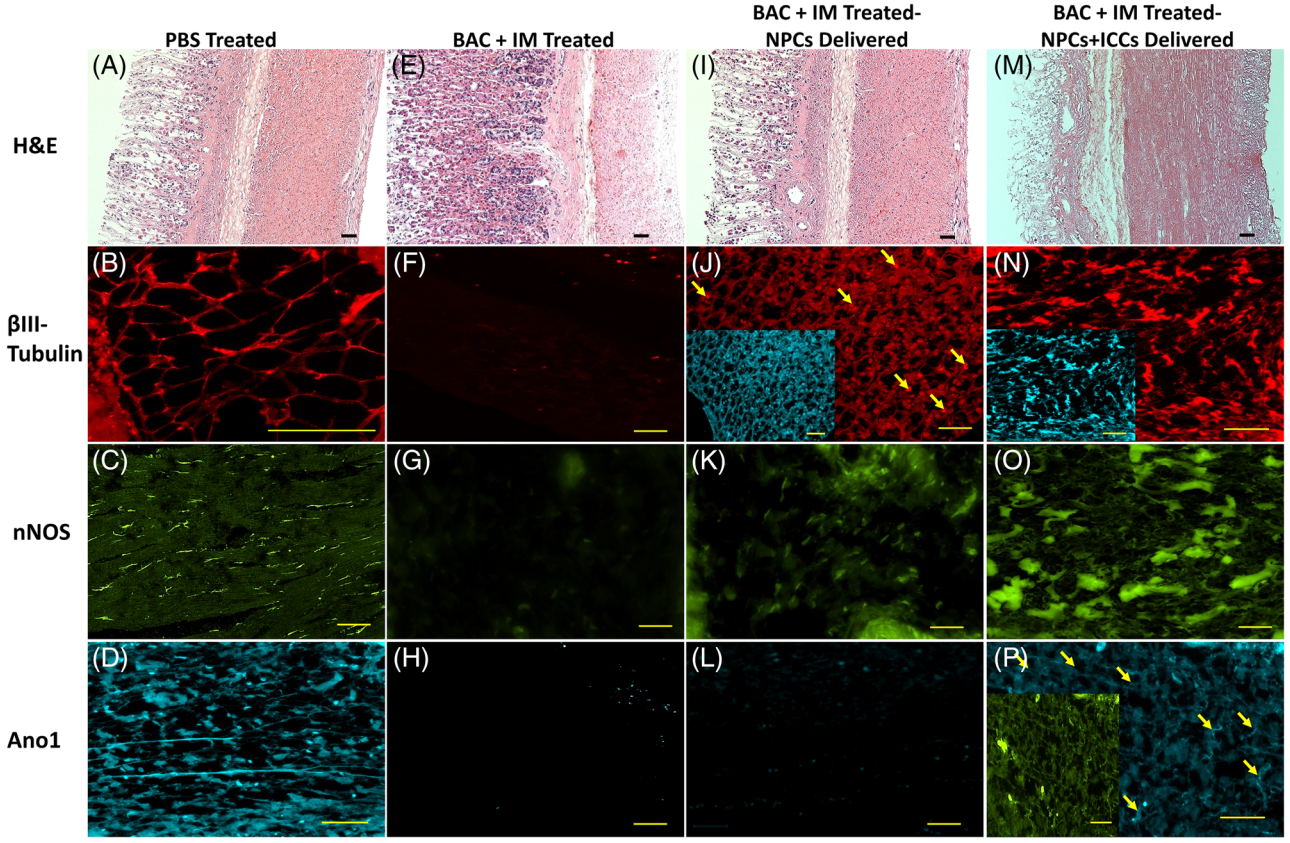

FIGURE 2 Immunocytochemistry and immunohistochemistry of tissues. A, E, I, and M. The H&E staining displayed a continual and intact serosa in all the tissues confirmed that BAC + IM did not affect the structural integrity of the outer layer; PBS-treated tissue displayed robust expression of B, βIII-tub; C, nNOS; and D, Ano1 indicated undamaged neurons and ICCs in the tissue. The BAC + IM-treated tissue showed ablation of F, functional neurons including G, nNOS and H, ICCs by poor expression to respective antibodies. J, The conjunction expression of CFP (in inset) with βIII-tub (in red) confirmed survival, differentiation, and innervation of injected NPCs in BAC + IM-treated tissues, the arrowhead represented undifferentiated circular shaped NPCs. K, The differentiated neurons displayed positive reactivity with nNOS neurons. L, The poor expression of Ano1 exhibited a limited self-regeneration of ICCs. N, The concomitant expression of CFP (in inset) and βIII-tub (in red) confirmed survival, differentiation, and innervation of injected NPCs with ICCs, without any significant undifferentiated cells. O, Differentiated neurons displayed robust reactivity with nNOS. P, The concomitant expression of GFP (in inset) and Ano1 (in Cyan) confirmed survival and differentiation of injected ICCs with NPCs, the arrowhead represented fusiform cell orientation of ICCs. Scale bar 100 μm. BAC, benzalkonium chloride; CFP, cyan fluorescent protein; GFP, green fluorescent protein; ICC, interstitial cells of Cajal; IM, imatinib mesylate; nNOS, neuronal nitric oxide synthase; NPC, neural progenitor cell; PBS, phosphate-buffered saline

3.4.2 | Biological characterization

The denervation and reinnervation were quantitatively analyzed using qPCR, where specific protein expressions for neuronal cells ($p75^{NTR}$, βIII-tub) and ICCs (ANO1) were evaluated. Compared with the PBS-treated group (βIII-tub: 24.5 ± 0.31; and ANO1: 28.3 ± 0.38), BAC + IM treatment exhibited a decrease in protein expression of βIII-tub (4.7 ± 0.24) and ANO1: (8.9 ± 0.35). It was a significant reduction in both βIII-tub (83%; P = .0012; n = 3) and ANO1 (67%; P = .0024; n = 3) compared with PBS-treated tissues (Figure 3A).

3.4.3 | Physiological functional characterization

The characteristic spontaneous basal tone generated by PBS-treated tissues (force: 298 ± 129 μN; area under the curve [AUC]: 186545 ± 3586) was reduced to an average minimum of (force: −66 ± 4.4 μN; AUC: −16 551 ± 57) after treatment of TMEM16A (ICC-specific calcium-activated chloride channel blocker). The basal tone in BAC + IM-treated tissues (force: 163.3 ± 53 μN; AUC: 105368 ± 4135; P = .0007; n = 3) was significantly low and did not exhibit any effect on TMEM16A treatment (Table 1).

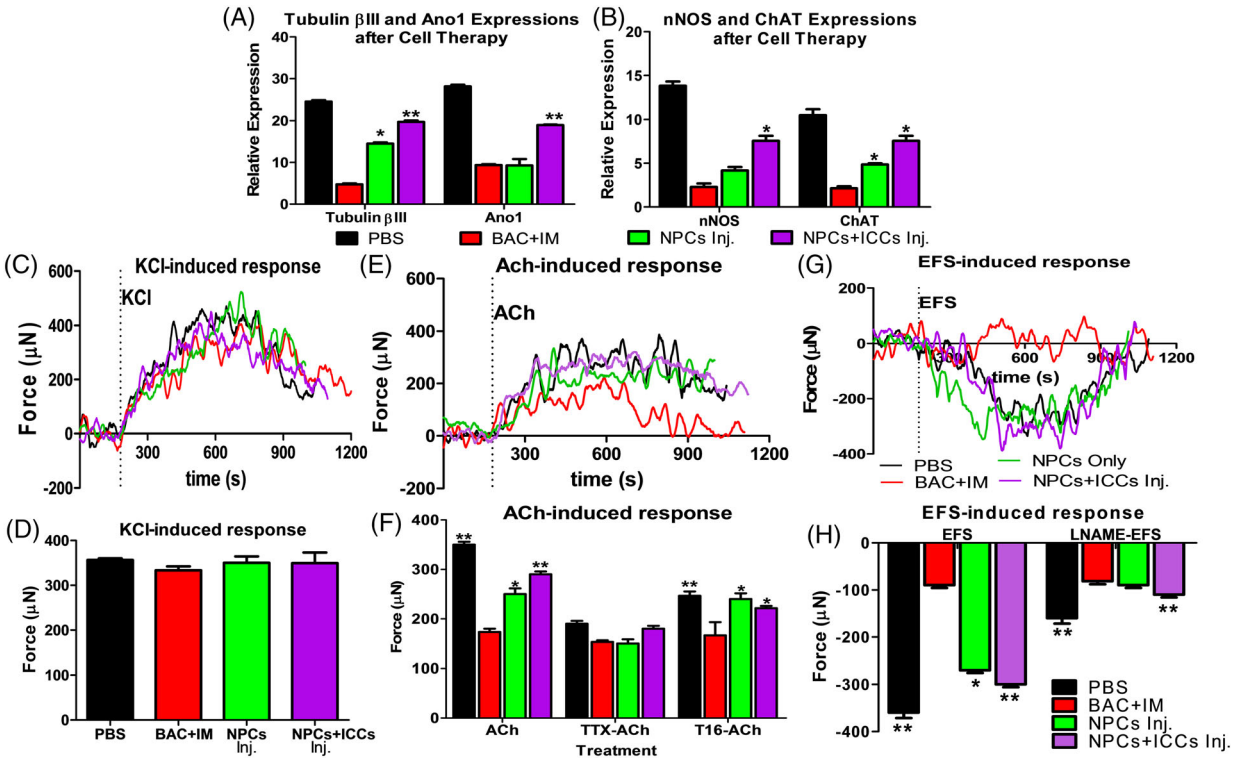

FIGURE 3 Restoration of functionality. A, Effects of cell injection on protein expression of βIII-tub and ANO1. The BAC + IM treatment resulted in significant loss of βIII-tub expression, the NPC + ICC-injected and NPC-injected tissues displayed significant improvement (P = .0004). NPC and ICC group expression of ANO1 showed improvement over the BAC + IM-treated tissue. Values shown as mean ± SEM (n = 3). B, The specific neural differentiation toward nNOS and ChAT expressions were also increased after cell injection. C and D, Summary of KCl-induced contractions suggest mild, nonsignificant differences in smooth muscle functionality in BAC + IM-treated, and cell-injected tissues, when compared with the PBS-treated tissue. E and F, Summary of ACh-induced contractions suggested significant differences in cholinergic responses among groups. Comparing ACh-induced contractions of PBS-treated tissue, the BAC + IM-treated tissue displayed loss of contraction (49.4%), whereas the NPC-injected group (P = .002; n = 3) and NPC + ICC-injected group (P = .001; n = 3) exhibited significant restoration of contraction. Pretreatment with tetrodotoxin (TTX, an inhibitor of voltage-gated Na + nerve channels) caused a decrease in ACh-induced contractile force in all groups except BAC + IM-treated tissue remained unaffected. Pretreatment with TMEM16A (T16, an ICC-specific calcium-activated chloride channel blocker) diminished contraction in the NPC + ICC-injected group (comparable to PBS-treated tissue) confirmed restoration of ICC-mediated contractions. G and H, Upon electrical field stimulation (EFS), rapid relaxation occurred in the PBS-treated tissues, NPC + ICC-injected tissues, and the NPC-injected tissues. EFS led to statistically significant relaxation in NPC + ICC-injected tissue (P = .001; n = 3) and NPC-injected tissue (P = .003; n = 3) compared with the PBS-treated tissue. The pretreatment of L-NAME (nNOS-specific blocker) led to diminished relaxation in the aforementioned groups, thus indicating the presence of functional nitrergic neurons. The summary graph of the force maximum of the area under the curve depicted in the bar graph. KCl, ACh, and EFS were directly applied to the organ bath at the dotted line. Values are shown as mean ± SEM. Each parameter value was obtained following a triplicate experiment with three independent tissue samples. * Values indicated P < .05 with BAC + IM treatment; **with NPC-injected treatment after BAC + IM treatment. ACh, acetylcholine; BAC, benzalkonium chloride; ChAT, choline acetyltransferase; ICC, interstitial cells of Cajal; IM, imatinib mesylate; L-NAME, N_{ω}-nitro-L-arginine methyl ester hydrochloride; nNOS, neuronal nitric oxide synthase; NPC, neural progenitor cell; PBS, phosphate-buffered saline

TABLE 1 Summary of physiological functional response in all groups

	KCl	ACh	TTX-ACh	T16-ACh	EFS	L-NAME-EFS	T16-Tone
PBS-treated (n = 3)							
Force ± SE	357 ± 5	350 ± 6	190 ± 6	247 ± 9	−360 ± 12	−160 ± 11	−95 ± 5
AUC ± SE	255 849 ± 1009	186 016 ± 363	113 561 ± 668	144 445 ± 2571	−144 711 ± 250	−64 453 ± 2065	−16 551 ± 57
BAC + IM-treated (n = 3)							
Force ± SE	300 ± 11.5	173 ± 7	153.3 ± 3.3	143.3 ± 3.3	−90 ± 6	−81.6 ± 6	−10 ± 5
AUC ± SE	195 874.3 ± 7283.6	116 354.6 ± 3035	101 694.3 ± 1404.3	110 047 ± 4442.1	−35 511.6 ± 9652.8	−32 454.3 ± 8494.1	−4891 ± 1415.8
ICC + NPC-injected (n = 3)							
Force ± SE	336 ± 9	290 ± 6	180 ± 6	221 ± 5	−300 ± 6	−110 ± 6	−100 ± 5
AUC ± SE	239 703.5 ± 15 205.5	177 393 ± 8833	110 982 ± 1477	133 677 ± 5750	−137 755.5 ± 6457.5	−57 544 ± 9740	−13 674.5 ± 2946.5
NPC-injected (n = 5)							
Force ± SE	350 ± 10	250 ± 20	150 ± 15	240 ± 20	−260 ± 20	−90 ± 10	−30 ± 10
AUC ± SE	239 351.0 ± 5354	159 689.0 ± 5431	105 046.0 ± 1350	140 983 ± 4567	−129 427.0 ± 5623	−53 122.0 ± 3987	5410.0 ± 1204

Abbreviations: ACh, acetylcholine; AUC, area under the curve; BAC, benzalkonium chloride; EFS, electrical field stimulation; ICC, interstitial cell of Cajal; IM, imatinib mesylate; L-NAME, N_{ω}-nitro-L-arginine methyl ester hydrochloride; NPC, neural progenitor cell; PBS, phosphate-buffered saline; SE, standard error; TTX, tetrodotoxin.

The treatment of potassium chloride (KCl, 60 mM) induced myogenic contraction primarily through depolarization of membrane[18] and confirmed the integrity and functionality of muscles. The PBS-treated tissue (force: 357 ± 5; AUC: 255849 ± 1009; n = 5) and BAC + IM-treated tissue (force: 336 ± 9; AUC: 222541 ± 6315; n = 5) produced a robust and rapid contraction. The results indicating that BAC + IM treatment did not affect SMCs functionality (Figure 3C,D) and preserved the calcium channels.

The neuron-mediated contraction was evaluated using ACh (1 μM). The PBS-treated tissues displayed strong contraction (force: 350 ± 8; AUC: 186016 ± 363; n = 5), which was reduced significantly (force: 190 ± 6; AUC: 113561 ± 668) on pretreatment potent neurotoxin TTX (40 μM). The ACh-induced contraction in BAC + IM-treated tissues (force: 173 ± 7 μN; AUC: 116354.6 ± 3035) was unaffected by TTX pretreatment (force: 153 ± 3 μN; AUC: 101694 ± 1404; P = .0002; n = 3). ACh-induced response generated through muscarinic receptors, which are present on both SMCs (M2R and M3R) and neurons (M1R).[16] The BAC + IM-treated tissues, resulted in significantly low (P = .0007; n = 3) contraction compared with PBS-treated tissues, and remained unaffected with TTX, validated the depletion of the neuronal population. Furthermore, this contraction was not affected by TTX validated the absence of neuronal population in the BAC + IM-treated tissues (Figure 3E,F). ACh-induced contraction was further evaluated with pretreatment of TMEM16A. The objective of this analysis was to evaluate the neuron-induced contraction mediated through ICCs. The PBS-treated tissues displayed an average maximum force of 247 ± 9 μN (AUC: 144445 ± 2571), which was remarkably (P = .0016; n = 3), low compared with ACh treatment due to ICC inactivity. This type of trend was absent after BAC + IM treatment, where tissues displayed 143 ± 3 μN (AUC: 110047 ± 4442), confirming depletion both of neurons and ICCs (Table 1).

EFS (5 Hz, 0.5 milliseconds) was used to evaluate neuron-evoked relaxation. EFS-induced excitation causes rapid and robust relaxation in PBS-treated tissues (force: −360 ± 12 μN; AUC: −144 610 ± 397; n = 3). The BAC + IM-treated tissue experienced a limited to nonexistent relaxation response in terms of force as well as magnitude (force: −90 ± 6 μN AUC: −35 511 ± 9652; n = 3; P = .0017) (Figure 3G,H). To confirm nNOS neurons, the tissues were pretreated with L-NAME (nNOS-inhibitor) prior to EFS stimulation. L-NAME treatment led to a significant decrease (green trace) in relaxation magnitude for PBS-treated tissues (force: −160 ± 11; AUC: −64 453 ± 2065), whereas BAC + IM-treated tissues were unaffected (Table 1). These results further confirmed inactivity and loss of neurons in the BAC + IM-treated tissues.

3.5 | Cell delivery and restoration of functionality

The PBS-treated tissue was kept as native tissue. The BAC + IM-treated tissues were divided into three groups. First group received 2 million NPCs/cm^3 in normal saline; second group received 2 million NPCs/cm^3 with 1 million ICCs/cm^3 in normal saline. The third group of tissues kept as diseased control, and only normal saline was injected. The injected cell population was optimized based on our previous studies.[19,20]

3.5.1 | Microscopic characterization

The immunohistochemical analysis displayed that injected fluorescent transduced cells survived, integrated, differentiated, and innervated at the site of injection without any migration. The fluorescent-tagged injected cells were visible at submucosal and muscular layers. The injected CFP-transduced NPCs (Figure 2J,N inset) stained positive against βIII-tub and confirmed differentiation into functional neurons in all cell-injected tissues (Figure 2J,N). The cell-delivered tissues displayed differentiation of NPCs and formation of reticulated neural population. The semi-quantitative histomorphometry analysis confirmed that 50% of neuronal network repopulated compared with BAC + IM-treated tissues.

The tissues injected with NPCs + ICCs exhibited higher differentiation compared with the tissues delivered with NPCs only. The pylorus tissues injected with NPCs without ICCs displayed undifferentiated circular shaped NPCs (arrowhead in Figure 2J) along with differentiated neural network. The histomorphometry analysis of images (three different tissues, three images of each tissue) of tissues concluded that coinjection of ICCs helped in NPCs differentiation and resulted in 38% ± 3% higher expression of βIII-tub.

A similar trend was evident in staining with a specific marker of nNOS. The sections of coinjected (NPCs + ICCs) tissues (Figure 2O) displayed significantly higher (P = .0312) nNOS expression compared with NPCs only (Figure 2K). The histomorphometry analysis of images confirmed 40% higher expression of nNOS in NPCs + ICCs co-injected tissues groups.

The concomitant expression of GFP and ANO1 in the cells delivered tissues, confirmed the survival and integration of ICCs in pylorus (Figure 2P). The NPCs + ICCs injected tissues displayed small fusiform cell orientation of ICCs (arrowhead in Figure 2P), which was absent in BAC + IM-treated tissues (Figure 2H) and NPC-injected tissues (Figure 2L).

3.5.2 | Biological characterization

After cell delivery, the ICC-injected tissues displayed significantly (34.4 ± 4.1%) upregulation in ANO1 expression (18.94 ± 0.5; P = .0004; n = 3) compared with the native expression of BAC + IM-treated tissues (8.9 ± 0.35) (Figure 3A).

Compared with denervated tissues, the βIII-tub expression was improved by 39.91% ± 2.5% after NPC delivery (14.53 ± 0.3; P = .0004; n = 3) and 61% ± 3.4% after the dual cell delivery (19.73 ± 0.22; P = .0004; n = 3) (Figure 3A). These results validated with $p75^{NTR}$ expression (undifferentiated NPCs), where the dual cells delivered tissues exhibited 35% higher neuronal differentiation compared NPCs only. The specific expression for nNOS in dual cell-injected tissues and NPC-injected tissues was 6.9 ± 0.33 and 4.6 ± 0.4, respectively (Figure 3B). These expressions confirmed restoration of ~50% nNOS population of the denervated tissues. The ChAT expression in dual cell-injected tissues and NPC-injected tissues was 7.55 ± 0.24 and 5.7 ± 0.28, respectively (Figure 3B).

3.5.3 | Physiological functional characterization

Physiological functional analysis was critical to determine the successful integration of delivered cells into the tissues (Table 1).

Basal tone

The dual cell-injected tissues exhibited the restoration of basal tone (force: 248.3 ± 27 μN; AUC: 155683 ± 9865). Similar to PBS-treated tissues, the treatment of TMEM16A reduced the basal tone (force: −100 ± 5 μN; AUC: −13 674 ± 2946) in dual cell-injected tissues, confirmed the restoration of ICCs functionality in the dual cell-injected tissues.

Electromechanical coupling integrity

The treatment with potassium chloride (KCl, 60 mM) induces myogenic contraction primarily through depolarization of membrane[18] and confirms the integrity and functionality of muscle. The NPC + ICC-injected tissues (force: 336 ± 9; AUC: 239703.5 ± 15 205; n = 3) and NPC-injected tissues (force: 350 ± 10; AUC: 239351 ± 5354; n = 3) produced a robust and rapid contraction, which was similar to the PBS-treated tissue (force: 357 ± 5; AUC: 255849 ± 1009; n = 5) and BAC + IM-treated tissue (force: 336 ± 9; AUC: 222541 ± 6315; n = 5). The results indicating that chemical treatment did not affect SMC functionality and preserved the calcium channels (Figure 3C,D).

Cholinergic response

After cell delivery, ACh induced a remarkable contraction response in both the NPC-injected group (force: 250 ± 20; AUC: 171689 ± 5431; n = 3), and the NPC + ICC-injected group (force: 290 ± 6; AUC: 177393 ± 8833; n = 3). Compared with native PBS-treated pylorus, there was 71% (P = .002) and 82% (P = .001) restoration of contraction in NPC-injected tissues and NPC + ICC-injected tissues, respectively. This reinstatement of contraction confirmed the differentiation of NPCs to functional neurons. The ACh-induced contraction following TTX pretreatment was significantly attenuated (red trace) in both NPCs delivered tissues (force: 250 ± 20; AUC: 159689 ± 5431; P = .0013; n = 3) and NPC + ICC-injected tissues (force: 290 ± 6; AUC: 177393 ± 8833; P = .0011; n = 3). This trend was similar yet lower to PBS-treated tissues (Figure 3E,F). It indicated that the contractile response in these tissues was mediated through both myogenic and neurogenic component.

The neuron-induced ICC-mediated contractions were studied with pretreatment with TMEM16A. The dual cell-injected group (force: 221 ± 5 μN; AUC: 133677 ± 5750) were similar to PBS-treated tissues (force: 247 ± 9 μN; AUC: 144445 ± 2571) owing to restoration of ICCs. This indicates that these tissues had ICCs mediating ACh-stimulated neuromuscular contractions, was absent in BAC + IM-treated tissues (force: 143 ± 3 μN; AUC: 110047 ± 4442; P = .0016; n = 3), or NPC-only injected tissues (force: 240 ± 20 μN; AUC: 150983 ± 4567; P = .0016; n = 3) (Figure 3F).

Neuron evoked relaxation

After cell injection, both the treated groups restored the relaxation response. The average maximum force generated by NPC + ICC-injected tissues (force: −300 ± 6; AUC: −137 755 ± 6457) was higher, but

AUC was not significantly different (P = .0011; n = 3) compared with NPC-injected tissues (force −260 ± 20; AUC: −129 427 ± 5623). Compared with native PBS-treated pylorus, there was 83%, (P = .001; n = 3), and 72% (P = .003; n = 3) reinstatement of relaxation in NPC + ICC-injected tissues and NPC-injected tissues, respectively. The EFS-induced relaxation in tissues is primarily through NO-mediated pathways (28). These results validated regeneration of relaxing nNOS expressing neurons in the cell-injected groups (Figure 3G,H).

To confirm nNOS neurons, the tissues were pretreated with L-NAME (nNOS-inhibitor) prior to EFS stimulation. L-NAME treatment led to a significant decrease (green trace) in relaxation magnitude for the NPC + ICC-injected group (force: −110 ± 6; AUC: −57 544 ± 9740) and NPC-injected group (force: −90 ± 10; AUC: −53 122 ± 3987) (Table 1). This attenuation of relaxation indicated the presence of functional nitrergic neurons. It confirmed that injected NPCs in all the cell-delivered groups differentiated to functional nitrergic neurons and functionally integrated with muscles.

4 | DISCUSSION

Normal pyloric motility depends on the coordinated activity of intrinsic and extrinsic neurons, SMCs, and ICCs.[21] The pylorus plays an important role in the gastric emptying process, the opening of the pylorus varies due to a modulation of the tonic activity of cells. Therefore, any irregularities affecting this coordinated process may give rise to abnormalities that differ according to the degree of damage. Depletion or dysfunction of one type of cells or different types of cells may result in pylorus dysmotility that contributes to delayed gastric emptying or gastroparesis. The simultaneous loss of both neurons and ICCs is almost universal in dysfunctionality and dysmotility of pylorus such as gastroparesis.[6,21]

The benefits of conventional treatment (medication and implantation of devices/inert materials) are temporary and provide symptomatic relief to most of the patients, whereas the surgical procedures (endoscopic myotomy) destroys the sphincter tone, and results are unpredictable as patients may develop rapid gastric emptying and dumping syndrome. Therefore, alternative approaches to pyloric therapies are needed. Regenerative medicine approach offers cellular replenishment by direct cell delivery. Human enteric NPCs were differentiated into neurons and glia after injection into aganglionic gut explants.[22] CNS-derived neural stem cells survived and differentiated into nNOS neurons after transplantations into the pylorus of mice.[15] Human embryonic or postnatal neurospheres like cells developed ganglia- like structures and enteric neurons after injection into aganglionic recipient guts of chick embryos.[23] The current cell therapy studies typically based on transplantation of neural stem cells or embryonic neural crest cells and not on adult enteric NPCs. Additionally, the network of ICCs is responsible for intrinsic pacemaker activity and also a critical intermediate between nerves and SMCs in organizing peristalsis and coordinate gastrointestinal motility.[17] Therefore, we developed a hypothesis that the simultaneous injection of ICCs and adult enteric NPCs cells could potentially improve survival of the cells as well as enhance the restoration of function to the diseased area.

In this objective, both ICCs and NPCs were isolated and demonstrated the appropriate morphology with genetic expression of the respective cell types. The dedifferentiation or loss of multipotent potential of NPCs in culture is challenging.[12,15] We demonstrated continual multipotent characteristics of our cultured NPCs as neurospheres. Subsequently, high-efficacy fluorescent tagging of the cultured cells was observed. These fluorescent protein-expressing cells were used for cell tracking studies after transplantation into the experimental tissues.

Previous studies on gastroparesis typically mimic the dysfunctionality through the application of BAC, which produces aganglionic conditions. But, neuropathy by itself does not constitute the typical situation encountered by gastroparesis patients. Gastroparesis is more accurately represented by the loss of both neurons and ICCs. It has found that BAC does not entirely obliterate ICC networks. To improve the accuracy of the ex vivo gastroparesis tissue model, BAC with IM were utilized during the chemical ablation of cells. Treatment of tissues with chemicals did not affect the structural integrity of the pyloric tissue nor damaged the smooth muscle, as demonstrated by H&E staining and KCl-induced contractions, respectively. Combined chemical treatment leads to the degradation of both neurons and ICCs.

This is the first report of co-delivery of ICCs and adult enteric NPCs in denervated dysfunctional pylorus tissues. In the present study, the immunoreactivity with neural differentiation marker in the co-injected group was 38% ± 3% higher compared with tissues delivered only NPCs without ICCs. It was further confirmed in qPCR studies, where injection of both cell types exhibited elevated expression of βIII-tub as a surrogate marker of neuron integration. This is consistent with other research which suggests that NPC and ICC co-transplantation promotes neuronal differentiation in aganglionic colon.[17] The extracellular matrix is vital for survival, colonization, migration, and replenishment of delivered neural stem cell in an aganglionated bowl. It has been reported that nonneuronal elements of an aganglionic region prevent the colonization and differentiation of neural crest cells.[24,25] Therefore, the presence of ICCs was critical for higher survival and differentiation of delivered NPCs. Compared with the delivery of enteric NPCs, the coinjection of duodenum-derived ICCs promoted differentiation of delivered NPCs in the denervated pylorus. These results indicated that the combination of ICCs to NPCs enhanced the efficacy of neuronal differentiation in an ex vivo denervated pylorus.

In the context of functionality, the contractile response to agonist-induced contraction and EFS-induced relaxation after cell delivery was successfully evoked and confirmed that the differentiated neurons were physiologically active and reinstated the functionality. The formation of synaptic connections between injected neural cells and native tissue was detected through diminished response to ACh upon inhibition of neurons in both cell-injected groups. However, ICC mediation of neurotransmission was demonstrated through decreased ACh-induced contraction through inhibition of ICCs in NPC + ICC-injected tissues. Relaxation was induced by blocking TMEM16A, confirmed the role of survival and functionality of ICCs in tissue tone.[18]

The importance of ICCs during functional development of ENS is yet to be proven. An in vitro study confirmed augmented differentiation of neural epithelial stem cells and intimate synapses with ICCs in rat aganglionic colon.[26] Recent reports suggested that the ENS-induced contractility is mediated through ICCs.[27] The higher force generation during ACh treatment compared with the pretreatment of TMEM16A inhibitor in dual cell-delivered tissues was consistent with the reported studies. These results indicated that neuronal evoked contractility is mediated through three different ways: (a) neuromodulator via muscle, (b) ICCs, and (c) neuronal interaction, compared with the classical synaptic neurotransmitter. The specific synapse formation between delivered NPCs and muscles or NPCs-ICCs needs to be investigated in detail.

The results of this study acknowledged as a short-term study due to the possibility of attrition of ex vivo tissues over longer period. But, the results can be useful to address neuromuscular dysfunctional diseases like gastroparesis in humans due to similarity in disease condition. The use of BAC + IM treatment model of neuromuscular dysfunctional pylorus as well as to the potential cell therapy efficacy can help pave the way toward a future treatment. In order to move this research toward translation to patient care, the next step would be to investigate NPCs and ICCs combination cell therapy on gastroparesis in vivo. In this endeavor, there are several challenges to overcome such as standardization of personalized cellular dosages, uniform distribution, and orientation of cells after injection, biodistribution, host cell integration, and long-term safety, without adverse effect such as fibrosis and tumorigenicity.

In summary, an ICC- and NPC-depleted ex vivo neuromuscular dysfunctional pylorus model was developed. The study demonstrated that simultaneous delivery of ICCs and NPCs could be used as an effective method to promote survival, differentiation, and integration of NPCs in a denervated and dysfunctional pylorus. The resulted reinstatement and restoration of functionality would be critical in the treatment of pylorus dysfunctionality. This preliminary study with the ex vivo diseased model proposed the next level of cell therapy for the treatment of gastroparesis.

ACKNOWLEDGMENTS

The authors acknowledge Suzanne Zhou and Dylan Knutson at Wake Forest Institute for Regenerative Medicine for helping in experimental work. This study was supported by NIH/NIDDK STTR R42DK105593 and Wake Forest School of Medicine Institutional Funds.

CONFLICT OF INTEREST

The authors declared no potential conflicts of interest.

AUTHOR CONTRIBUTIONS

K.B.: conceptualized and designed the study, provided study supervision, administration, and funding, reviewed the manuscript; P.D.: conceptualized and designed the study, carried out the experimental work, carried out biological experiments, microscopic characterized, data acquisition, analyzed the physiology data, wrote the manuscript, reviewed the manuscript.

DATA AVAILABILITY STATEMENT

The data that support the findings of this study are available from the corresponding author upon reasonable request.

ORCID

Prabhash Dadhich https://orcid.org/0000-0002-1631-6240

REFERENCES

1. Camilleri M, Parkman HP, Shafi MA, Abell TL, Gerson L. Clinical guideline: management of gastroparesis. *Am J Gastroenterol*. 2013;108(1):18-38.
2. Patrick A, Epstein O. Review article: gastroparesis. *Aliment Pharmacol Ther*. 2008;27(9):724-740.
3. Jung H, Choung RS, Iii GRL, et al. The incidence, prevalence and outcomes of patients with gastroparesis in Olmsted County, Minnesota from 1996 to 2006. *Gastroenterology*. 2009;136(4):1225-1233.
4. Kashyap P, Farrugia G. Diabetic gastroparesis: what we have learned and had to unlearn in the past 5 years. *Gut*. 2010;59(12):1716-1726.
5. Iwasaki H, Kajimura M, Osawa S, et al. A deficiency of gastric interstitial cells of Cajal accompanied by decreased expression of neuronal nitric oxide synthase and substance P in patients with type 2 diabetes mellitus. *J Gastroenterol*. 2006;41(11):1076-1087.
6. Grover M, Farrugia G, Lurken MS, et al. Cellular changes in diabetic and idiopathic gastroparesis. *Gastroenterology*. 2011;140(5):1575-1585.
7. Sivarao DV, Mashimo H, Goyal RK. Pyloric sphincter dysfunction in nNOS−/− and W/Wv mutant mice: animal models of gastroparesis and duodenogastric reflux. *Gastroenterology*. 2008;135(4):1258-1266.
8. Shah V, Lyford G, Gores G, Farrugia G. Nitric oxide in gastrointestinal health and disease. *Gastroenterology*. 2004;126(3):903-913.
9. Choi KM, Gibbons SJ, Roeder JL, et al. Regulation of interstitial cells of Cajal in the mouse gastric body by neuronal nitric oxide. *Neurogastroenterol Motil*. 2007;19(7):585-595.
10. McCallum RW, Snape W, Brody F, Wo J, Parkman HP, Nowak T. Gastric electrical stimulation with Enterra therapy improves symptoms from diabetic gastroparesis in a prospective study. *Clin Gastroenterol Hepatol*. 2010;8(11):947-954.e1.
11. Zarate N, Mearin F, Wang X-Y, et al. Severe idiopathic gastroparesis due to neuronal and interstitial cells of Cajal degeneration: pathological findings and management. *Gut*. 2003;52(7):966-970.
12. Pan WK, Zheng BJ, Gao Y, Qin H, Liu Y. Transplantation of neonatal gut neural crest progenitors reconstructs ganglionic function in benzalkonium chloride-treated homogenic rat colon. *J Surg Res*. 2011;167(2):e221-e230.
13. Hotta R, Stamp LA, Foong JPPP, et al. Transplanted progenitors generate functional enteric neurons in the postnatal colon. *J Clin Invest*. 2013;123(3):1182-1191.
14. Burns AJ, Goldstein AM, Newgreen DF, et al. White paper on guidelines concerning enteric nervous system stem cell therapy for enteric neuropathies. *Dev Biol*. 2016;417(2):229-251.
15. Micci MA, Learish RD, Li H, Abraham BP, Pasricha PJ. Neural stem cells express RET, produce nitric oxide, and survive transplantation in the gastrointestinal tract. *Gastroenterology*. 2001;121(4):757-766.
16. Gilmont RR, Raghavan S, Somara S, Bitar KN. Bioengineering of physiologically functional intrinsically innervated human internal anal sphincter constructs. *Tissue Eng Part A*. 2014;20(11–12):1603-1611.
17. Zhang L, Zhao B, Liu W, Ma R, Wu R, Gao Y. Cotransplantation of neuroepithelial stem cells with interstitial cells of Cajal improves neuronal differentiation in a rat aganglionic model. *J Pediatr Surg*. 2017;52(7):1188-1195.
18. Ward SM, Mclaren GJ, Sanders KM. Interstitial cells of Cajal in the deep muscular plexus mediate enteric motor neurotransmission in the mouse small intestine. *J Physiol*. 2006;573(Pt 1):147-159.

19. Rego SL, Zakhem E, Orlando G, Bitar KN. Bioengineered human pyloric sphincters using autologous smooth muscle and neural progenitor cells. *Tissue Eng Part A*. 2016;22(1–2):151-160.
20. Rego SL, Raghavan S, Zakhem E, Bitar KN. Enteric neural differentiation in innervated, physiologically functional, smooth muscle constructs is modulated by bone morphogenic protein 2 secreted by sphincteric smooth muscle cells. *J Tissue Eng Regen Med*. 2017;11(4):1251-1261.
21. Sanders KM, Koh SD, Ro S, Ward SM, Weaver A. Regulation of gastrointestinal motility—insights from smooth muscle biology. *Nat Rev Gastroenterol Hepatol*. 2012;9(11):633-645.
22. Almond S, Lindley RM, Kenny SE, Connell MG, Edgar DH. Characterisation and transplantation of enteric nervous system progenitor cells. *Gut*. 2007;56(4):489-496.
23. Metzger M, Caldwell C, Barlow AJ, Burns AJ, Thapar N. Enteric nervous system stem cells derived from human gut mucosa for the treatment of aganglionic gut disorders. *Gastroenterology*. 2009;136(7):2214-2225.
24. Rothman TP, Goldowitz D, Gershon MD. Inhibition of migration of neural crest-derived cells by the abnormal mesenchyme of the presumptive aganglionic bowel of is/is mice: analysis with aggregation and interspecies chimeras. *Dev Biol*. 1993;159(2):559-573.
25. Jacobs-Cohen RJ, Payette RF, Gershon MD, Rothman TP. Inability of neural crest cells to colonize the presumptive aganglionic bowel of ls/ls mutant mice: requirement for a permissive microenvironment. *J Comp Neurol*. 1987;255(3):425-438.
26. Zhao B, Liu W, Wu R. Co-culture of neuroepithelial stem cells with interstitial cells of Cajal results in neuron differentiation. *Int J Clin Exp Med*. 2015;8(7):10437-10443.
27. Sanders KM, Koh SD, Ward SM. Interstitial cells of Cajal as pacemakers in the gastrointestinal tract. *Annu Rev Physiol*. 2006;68(1):307-343.

SUPPORTING INFORMATION

Additional supporting information may be found online in the Supporting Information section at the end of this article.

How to cite this article: Dadhich P, Bitar KN. Functional restoration of ex vivo model of pylorus: Coinjection of neural progenitor cells and interstitial cells of Cajal. *STEM CELLS Transl Med*. 2020;9:713–723. https://doi.org/10.1002/sctm.19-0316